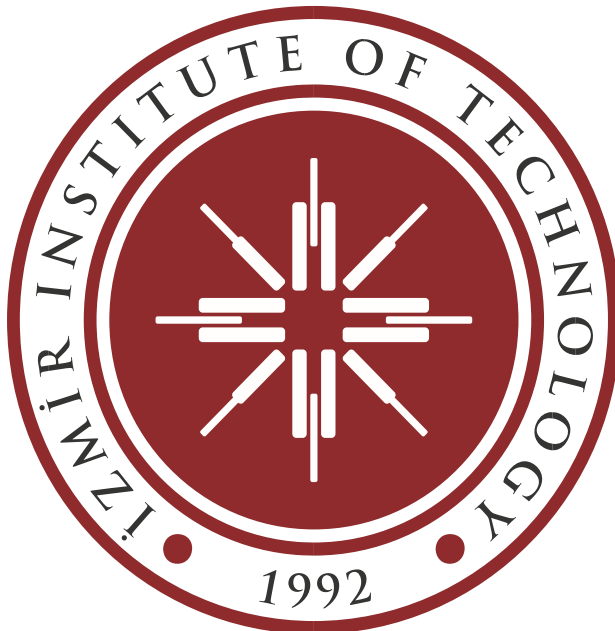


Sending Image and Text Using Software Defined Radio

EE453-Project



Group Members:

Behiye Erdemir - 240206013

Polat Altunbağ - 240206054

Furkan Ayberk Yağdı - 240206032

Esin Sanem İmamoğlu - 240206006

Content

CONTENT OF TABLES	4
1. INTRODUCTION.....	6
2. TRANSMITTER	8
2.1 CODING	8
2.2 PULSE SHAPING	8
2.2 ANALOG UPCONVERSION	9
3. CHANNEL.....	10
4. RECEIVER.....	11
4.1 RECEIVER ANTENNA.....	11
4.2 BANDPASS FILTER AND AUTOMATIC GAIN CONTROL.....	11
4.3 DIGITAL DOWNCONVERSION AND CARRIER SYNCHRONIZATION.....	14
4.4 CORRELATOR	16
4.5 DOWNSAMPLING AND TIME SYNCHRONIZATION	17
4.6 DECISION	20
4.7 DECODING	21
5. RESULTS	22
5.1 IDEAL SYSTEM.....	22
5.2 TEST FOR EASY CONDITIONS	23
5.3 TEST FOR MEDIUM CONDITIONS.....	25
5.4 TESTS FOR HARSH CONDITIONS	26
5.4 TESTS FOR EXTREME CONDITIONS	28
6. CONCLUSION.....	29
REFERENCES	30

Content of Figures

Figure 1: Block-chart of the designed system	7
Figure 2: Zero padded message signal	8
Figure 3: Baseband message signal that is shaped with Hamming pulse	9
Figure 4: Suppressed carrier modulated signal with frequency of 70 Hertz.....	9
Figure 5: Effect of BPF with Gaussian noise with variance = 1, and flat fading with gain = 0.5	12
Figure 6: Sampling with Automatic Gain Control using adaptive parameter gain a	12
Figure 7: Magnitude compensation of AGC in the presence of flat fading with gain = 0.5	13
Figure 8: Convergence of the phase tracking.....	15
Figure 9: Cost function for decision directed method	15
Figure 10: Convergence of phase tracking by decision directed method, initial estimates -0.7 and 0.7 respectively while phase offset is -1	16
Figure 11: Effect of the correlator.....	16
Figure 12: Eye diagrams at the input and the output of the correlator.....	17
Figure 13: Convergence of the time offset	18
Figure 14: Convergence of the time offset with output power maximization method	19
Figure 15: Effect of the flat fading on time recovery	19
Figure 16: Labels the signals at various points [7] .	20
Figure 17: Transmitted and received images	21
Figure 18: Soft and Hard decisions.....	23
Figure 19: Transmitted and received images	23
Figure 20: Soft and Hard decisions.....	24
Figure 21: Transmitted and received images	25
Figure 22: Soft and Hard decisions.....	26
Figure 23: Transmitted and received images	26
Figure 24: Soft and Hard decisions.....	27
Figure 25: Transmitted and received images	27
Figure 26: Soft and Hard decisions.....	28
Figure 27: Transmitted and received images	29

Content of Tables

Table 1	22
Table 2	22
Table 3	24
Table 4	24
Table 5	25
Table 6	25
Table 7	26
Table 8	27
Table 9	28
Table 10	28

Content of Equations

Eq. 1	11
Eq. 2	12
Eq. 3	12
Eq. 4	13
Eq. 5	14
Eq. 6	14
Eq. 7	14
Eq. 8	14
Eq. 9	15
Eq. 10	17
Eq. 11	18
Eq. 12	19
Eq. 13	20
Eq. 14	20
Eq. 15	20
Eq. 16	20
Eq. 17	21
Eq. 18	21

1. Introduction

The widespread usage of analog-to-digital converters (ADC) with developing samplers and the development of software tools used in modern communications; the hardware components used in communication systems have been replaced by software-based techniques because they are easy to implement, fast, and cheap.

Software-defined radio (SDR) is a type of wireless communication in which a computer generates or defines the transmitter modulation [1]. In digital radio, processing of baseband signal is always performed on a digital processor. In software radio, antenna output is sampled in a direct way. It is a wireless enabling technology that can be used in a variety of applications and provides flexible, upgradeable, and longer-lasting radio equipment with more adaptable and probably less expensive multi-standard interfaces [2].

SDR simply is a radio having some of all of the physical layers are software-defined [3]. The operation of an SDR is based on the idea of analog and digital parts functioning together since the electromagnetic wave transmitted in the air is analog.

In our project, a text or an image is sent using the software defined radio. Signal is converted to sequence of bits with magnitudes +1, -1, +3, -3. After that, Amplitude modulation with suppressed carrier is used to perform Analog Upconversion to be able to send bits through the medium, air for radio communication. Combining pulses with Amplitude modulation, 4-level PAM is used to transmit signal. Channel is examined with the effects of Broadband, Narrowband noise, and Flat fading.

Block-chart of the project can be seen in **Figure 1**, our aim is adapting Phase synchronization, Time synchronization (for pulse timing offset), and overcoming challenges of noises and flat fading by using Bandpass filter, and Automatic Gain Control. Also, convolution is used in Correlator in order to recover last symbol in the signal. It clarifies pulses and enables correct timing in Down Sampler by knowing where to sample exactly to recover the transmitted bits. After down sampling, decision block gives hard decisions. At the end, if a text is sent, decoding is performed to reconstruct message from hard decided bits using ASCII coding again. If an image is sent, decoding using ASCII is not required, instead bits are grouped in 8. Grouped bits are converted to decimal, since an image have pixel value range between 0 and 255. Lastly, reshaping is applied to recover the image.

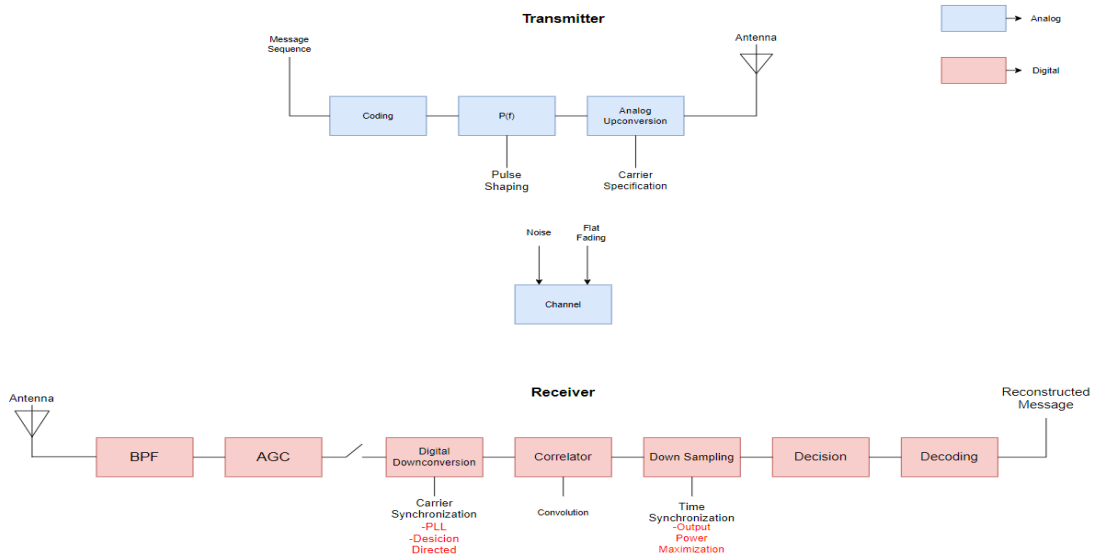


Figure 1: Block-chart of the designed system

As indicated in the diagram, we tried to realize the system by overcoming challenges above, using most of the blocks that we learned. Even it is not indicated in the block diagram, adaptive receiver gain is implemented to calculate signal power, like it is explained section 4.2, that is used in AGC instead of assuming power content is known. Also, received signal is pre-processed before Digital Conversion block, where PLL and Decision Directed is implemented, in order to extract carrier information since suppressed carrier is used in modulation.

2. Transmitter

2.1 Coding

In our project, our aim is sending text and image. Firstly, in order to send text, it is converted to stream of bits using ASCII code, 8 bits per character. After that, bits are grouped in two and they are scaled in to pulses with magnitudes +1, -1, +3, -3 in order to implement 4 level PAM with 4 symbols. Secondly, in order to send the image, conversion using ASCII is not needed since each pixel in a colored image have values between 0 and 255 for each color dimension. Each pixel value is represented with 8-bits already for red, green, and blue colors by converting decimal to binary. Three dimensions are flattened and each pixel value is converted to bits. After that, 4 level PAM is used to send image again. Assuming an image that contains r rows, and c columns, transmission results in sending $(r \times c \times 3 \times 8)$ bits.

2.2 Pulse Shaping

Pulse shaping is making the signal suitable for the frequency band and applied for each symbol. Narrow pulses in time may provide faster transmission but in frequency band they create interference as it can be seen in **Figure 2**. This step reduces inter symbol interference and provides effective use of bandwidth for the transmission.

In this project, hamming window is used as a pulse shaping filter with 200 window samples. Before applying filter, in order to make space for this window, signal is constructed with zero padding as shown in **Figure 2**.

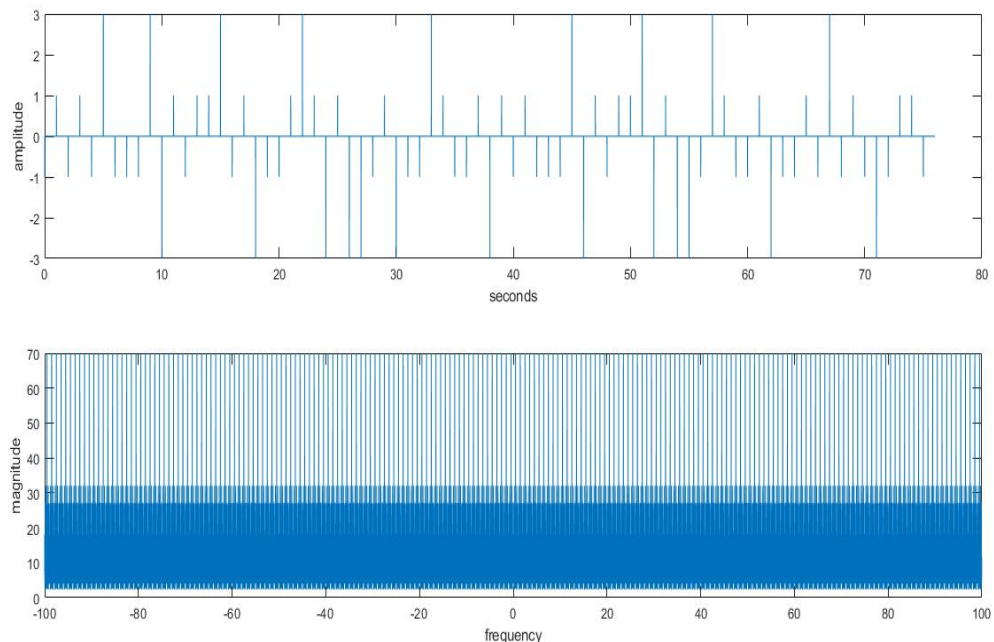


Figure 2: Zero padded message signal

Then, in **Figure 3** Hamming pulse shaped message signal is shown. This shows frequency interferences are mostly prevented even if there are small interferences. Signal is become suitable for transmission this way.

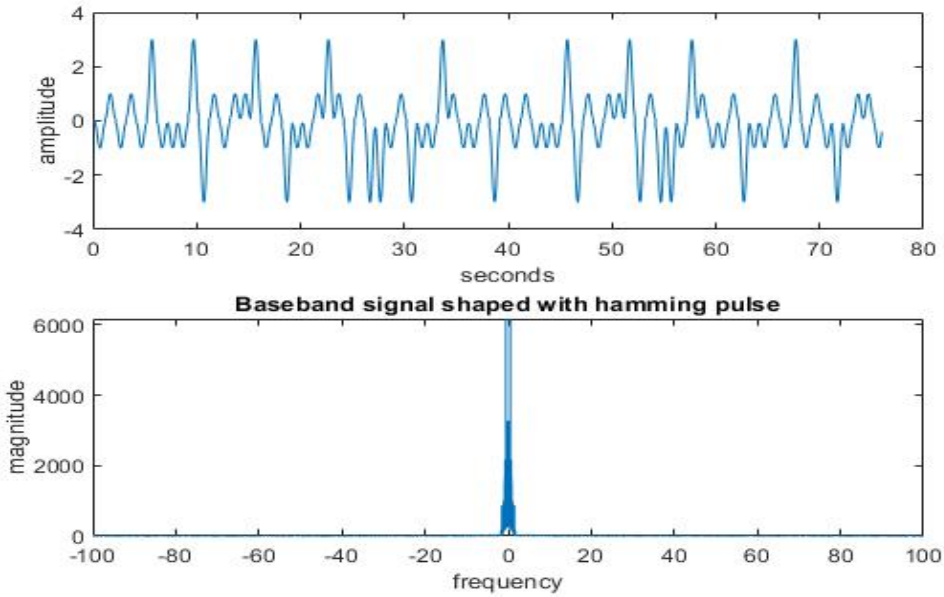


Figure 3: Baseband message signal that is shaped with Hamming pulse

2.2 Analog Upconversion

Radio communication uses air as the transmission medium and transmitting the signal through long distances require specification of a carrier. In our project, Amplitude modulation with the suppressed carrier is used with 70 Hertz as can be seen in **Figure 4**. It is selected low for the purpose of easier observation during project development.

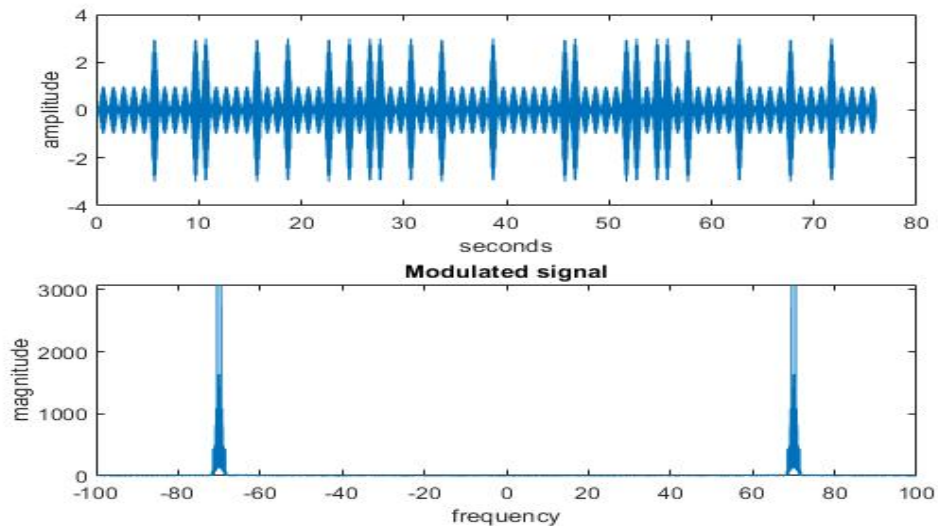


Figure 4: Suppressed carrier modulated signal with frequency of 70 Hertz

3. Channel

In reality, there are different conditions that results in corruption of the communication model like noise, multipath effects, user interferences, channel gain. In order to create a successful communication model, it is a necessity to prevent such effects that may cause the system to corrupt. In our project, channel effect is examined with the presences of Broadband noise, Narrowband noise and Flat Fading.

Transmitted information is conveyed through air in radio communication, while the signal is taking its path, it faces distortions that makes it much harder to receive. Broadband noise is one of challenges that should be reduced because it exists in everywhere since it is a background noise. Reducing the effect of Broadband noise is achieved by implementing a bandpass filter around the corner frequency of the carrier signal, which is 70 Hertz. Also, lots of different systems operate in same frequency spectrum as the communication systems, and applying bandpass filter and a notch filter can provide more accurate communication even if notch filter can degrade some portion of the signal since its bandwidth is comparably small with respect to signal to be transmitted.

Fading is frequently encountered effect due to weather conditions or surrounding structures. Multipath interference is another important issue that should be worked on even if it is not included in our project. Transmitted signal takes different paths until it reaches the receiver. Signal reflects from surrounding objects that have different absorption and reflection properties, and takes paths with different lengths, so it creates fluctuations in magnitude with changing timing. This channel effect can be modelled as a filter with a channel response, so it can be inverted using an inverse filter with equalization. Since radio communication is wireless, signal is exposed to attenuation that results in fading like Multipath effect, and Flat fading is a type of Multipath.

For the case of flat fading, coherence bandwidth, where fading effect takes part, of the channel bandwidth is larger than the signal bandwidth [4]. In this situation, all frequency components in the signal faces same amount of fading effect. Automatic Gain Control is used to recover signal magnitude with the idea of preserving power content of the signal. Flat fading is modelled as reduction in magnitude directly in our project. Effect of channel gain is generally observed with three different values, which are 0.8, 0.5, 0.2 times of magnitude of the original signal to test the different conditions like small, average or harsh fading effects.

4. Receiver

Communication systems are getting more based on software with the increased sampling power, and reducing cost, basically with improving efficiency as a result of development in technology. Software defined communication is desired because of the ease in signal processing, reduced cost, and adaptive structure. Since software is the direction of communication recently, we wanted to realize the system as much as possible.

4.1 Receiver Antenna

Power content of a signal is important to implement Automatic Gain control to compensate the effect of Flat fading. In order to achieve a more realized system, we implemented adaptive receiver antenna gain to calculate power content of the transmitted signal instead of assuming power of the signal is transmitted directly. In wireless communication, received power depends on four variables. First one is Effective isotropic radiated power, which is a power measurement that represents the power radiated by an isotropic transmitter antenna as equal strength with original signal. Also, received power depends on signal frequency, net bit-rate and receiver antenna gain as it can be seen in the **Equation 1** [5].

$$P_r = \frac{EIRP}{\left(\frac{4\pi}{\lambda}\right)R^2} G_R \quad \text{Eq. 1}$$

R: Net bit-rate, G_R: Receiver gain, EIRP: Effective isotropic radiated power

4.2 Bandpass Filter and Automatic Gain Control

Firstly, Bandpass filter is used at the front-end of the receiver in order to eliminate broadband and narrowband noises. Broadband noise presents through all frequency ranges, eliminating out-of-band portion of the noise increases Signal-to-noise ratio of received signal by reducing noise power even if signal power is not changed. Remaining broadband noise is mostly tolerated by hard decision at the end. Notch filter is not implemented to do not degrade the received signal, this way to observe working of remaining parts in the system better. Effect of bandpass filter on SNR can be understand visually by looking results in **Figure 5**.

As it can be seen in the results in **Figure 5**, out-band portion of the broadband noise, and random narrowband pulses are eliminated. Also, starting from approximately 30th second, flat fading reduces magnitude of the signal and Automatic Gain Control must be used to compensate this channel gain.

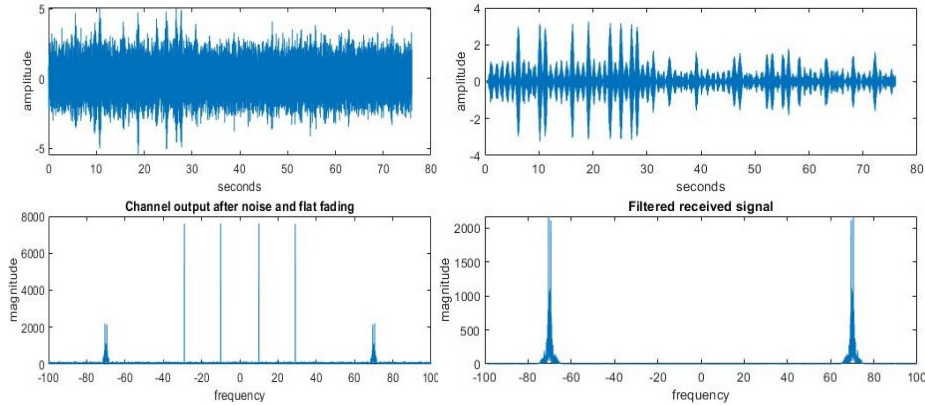


Figure 5: Effect of BPF with Gaussian noise with variance = 1, and flat fading with gain = 0.5

Samplers have operation range specifications for every condition like magnitude, temperature, frequency, timing etc. like every device. Proper working of the system requires fixing dynamic range of received signal amplitude to perform analog to digital conversion. Since channel effects can change magnitude of the signal drastically, Automatic Gain Control is used to compensate channel gain that comes with flat fading. Automatic Gain Control provides proper sampling by multiplying received signal with gain factor a that can be seen on the **Figure 6**. Sampling with AGC is implemented based on Gradient descent approach, which is commonly used in optimization procedures in many areas.

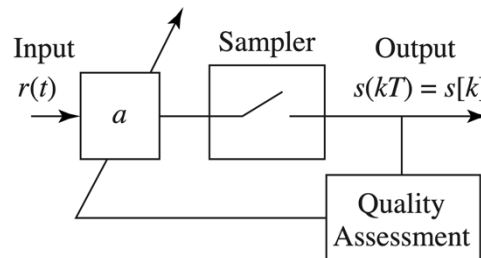


Figure 6: Sampling with Automatic Gain Control using adaptive parameter gain a

Gradient descent algorithm is based on optimization (minimization for our case) of a cost function in general, where cost function defines the desired behaviour of any system. In this project, minimization of cost function with steepest descent corresponds to reducing power difference between the original signal and received signal samples in the optimum way with the window of predefined length.

$$J(a) = \left(\frac{1}{4}\right) \text{avg}(a^2 r^2[k] - S^2) \quad \text{Eq. 2}$$

$$a[k + 1] = a[k] - \mu \frac{d(J(a))}{dt} \quad \text{Eq. 3}$$

This algorithm provides converge to the original signal magnitude level with the adjustment of gain parameter a , and this way, dynamic range of the signal is kept in the operation range of the sampler. Using differentiation, if power of received signal samples are smaller than S^2 , system increases gain parameter a with a rate defined by step size μ since differentiation result becomes negative. Magnitude of the received samples are amplified with large gain and fading effect is compensated. If power of received signal samples are larger than predefined S^2 , differentiation becomes positive and gain a is reduced, this way magnitude of received samples are attenuated.

Final form of algorithm, which is used in the project, is achieved by inserting differentiation of cost function in **Equation 2** to **Equation 3** and it can be seen in the **Equation 4**.

$$a[k + 1] = a[k] - \mu avg(sgn(a[k])(s[k]^2 - S[k]^2)) \quad \text{Eq. 4}$$

Step size μ is an important parameter to achieve converge. Large step size can result with fail of convergence since there is possibility to pass the minimum point in the cost function. Also, very small step size creates slow convergence, which is not wanted in real time systems. In our project, step size is selected to be 0.001 and sample size to perform averaging operation as window is selected as 10. Effect of AGC can be seen in the **Figure 7**. It is suitable to compensate effect of flat fading.

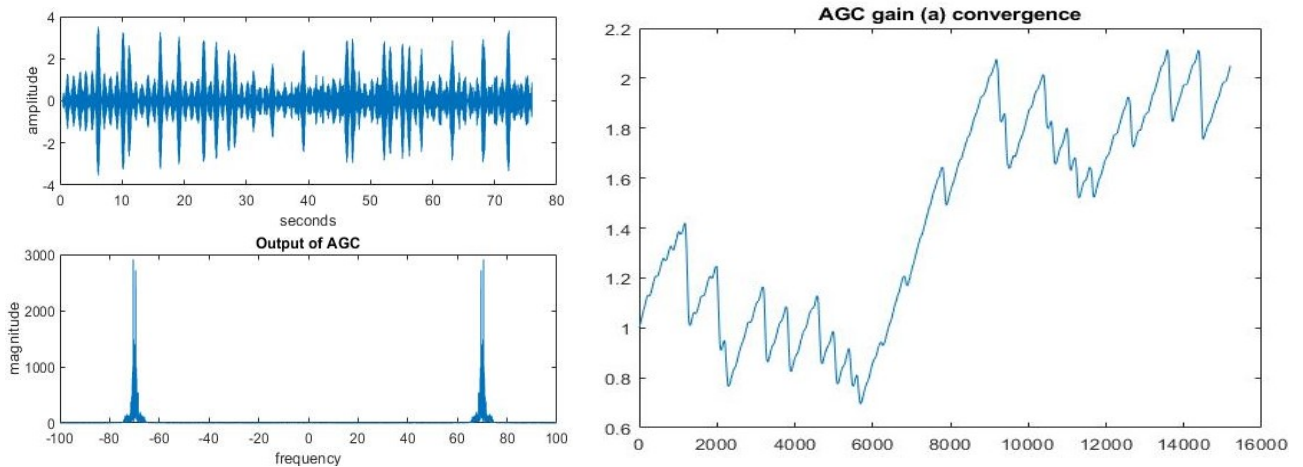


Figure 7: Magnitude compensation of AGC in the presence of flat fading with gain = 0.5

Comparing **Figure 7** and **Figure 5** it can be seen that, magnitude is recovered to the levels +1, -1, +3, and -3. Flat fading is starting at 30th second, so AGC gain is increasing to 2 to compensate 0.5 channel gain. Small spike shapes in AGC gain convergence figure are because of constant magnitude changes in PAM, and effect of noise.

4.3 Digital Downconversion and Carrier Synchronization

Phase information of the received signal is generally different from the original signal even if phase information is provided to the receiver from transmitter. There are different reasons that can create phase difference between transmitted and received signal like oscillators error margins, jitters, different path length in Multipath etc. After AGC block, received signal must be processed before phase synchronization, since AM with suppressed carrier is used to modulate baseband signal. This processing is applied to perform Carrier extraction, and it is implemented by bandpass filtering the squared received signal.

In the ideal communication system, the receiver receives a baseband component by multiplying the incoming signal with a sinusoidal. The desired signal is obtained by passing this signal through a lowpass filter. But in non-ideal (real) systems, the receiver and transmitter do not have the same carrier phase and frequency. Several methods can be used for this, phase-locked loop and decision directed methods are used in this project. In order to obtain the minima in cost function, adaptive systems using the steepest descent method are implemented. The phase-locked loop method has low computational complexity but requires pre-processing. Since we have the received signal as;

$$r(t) = s(t) * \cos(2\pi f_c t). \quad \text{Eq. 5}$$

Signal is processed so that the carrier phase component appears as in large carrier modulation. It is possible to get the carrier information when the signal is squared and passed through a narrow bandpass filter that is why it is called pre-processing. Then obtained signal is;

$$r^2(t) = \frac{1}{2} * s^2(t) * [1 + \cos(4\pi f_c t + 2\phi)]. \quad \text{Eq. 6}$$

When a narrow bandpass filter centered at $2f_c$ is used, then we obtain;

$$r(t) = \frac{1}{2} * s_{avg}^2 * [\cos(4\pi f_c t + 2\phi)]. \quad \text{Eq. 7}$$

In addition, the bandpass filter phase is neglected since it is known at the receiver side and it is small enough to be ignored.

The simple logic behind the PLL (Phase-Locked Loop) method is; pre-processed signal is multiplied with the local oscillator and pass it through the lowpass filter, carrier phase estimation can be achieved from the cosine function that appears in **Equation 8**;

$$\left(\frac{s_{avg}^2}{2}\right)/4 * \cos(2\phi - 2\theta). \quad \text{Eq. 8}$$

This process is used to find the phase of the incoming signal by taking the derivative of the phase in the local oscillator. So, the final approach is seen in **Equation 9**;

$$\theta[k+1] = \theta[k] - \mu LPF\{r_p(kT_s) \sin(4\pi f_0 k T_s + 2\theta[k] + \psi)\}. \quad Eq. 9$$

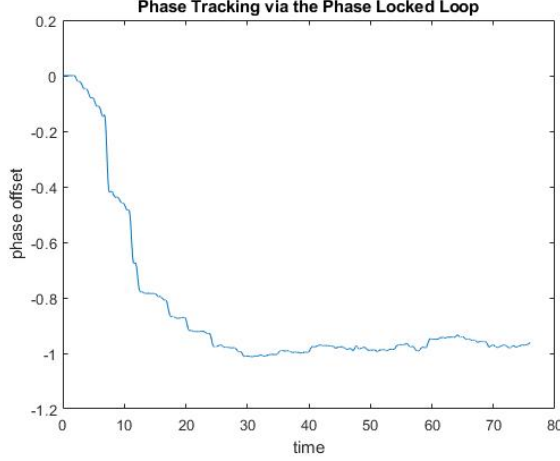


Figure 8: Convergence of the phase tracking

As can be seen in the **Figure 8**, the algorithm converges to -1 while our initial phase estimation is 0 and our actual phase offset was -1. The reason why the signal is not smooth is that it is taken from a noise-containing channel and pre-processed.

Our other method is the decision directed method. The logic of this method is based on the difference between soft and hard decision values. It turns the reflection of the difference in $\cos(2\Phi-2\theta)$ obtained after applying carrier extraction to these two decisions to an advantage. The aim is to choose the phase that will minimize the difference between these two decisions.

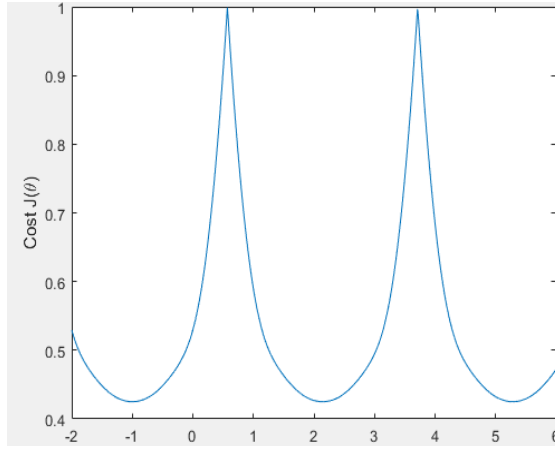


Figure 9: Cost function for decision directed method

While our phase offset is -1, the cost function we obtained in the decision direct method is as in **Figure 9**. As it is predicted, minimum is obtained when the phase offset was at -1 and its replicas. The advantage of this method is that it does not need any pre-processing, it does not require anything extra to estimate the phase according to the difference between the hard and soft decisions of the symbols while trying to recover the symbols. But the biggest

disadvantage is that it is affected by the initial value estimation of phase, so initial estimation value should be close to the real phase offset. As can be seen in the **Figure 10**, when the phase offset is -1 and the initial phase offset estimate is given as -0.7, a correct convergence is achieved, but when the initial phase estimation is given as +0.7, the algorithm works incorrectly and converges to approximately 2, as it is expected looking at the cost function with more than one local minima values.

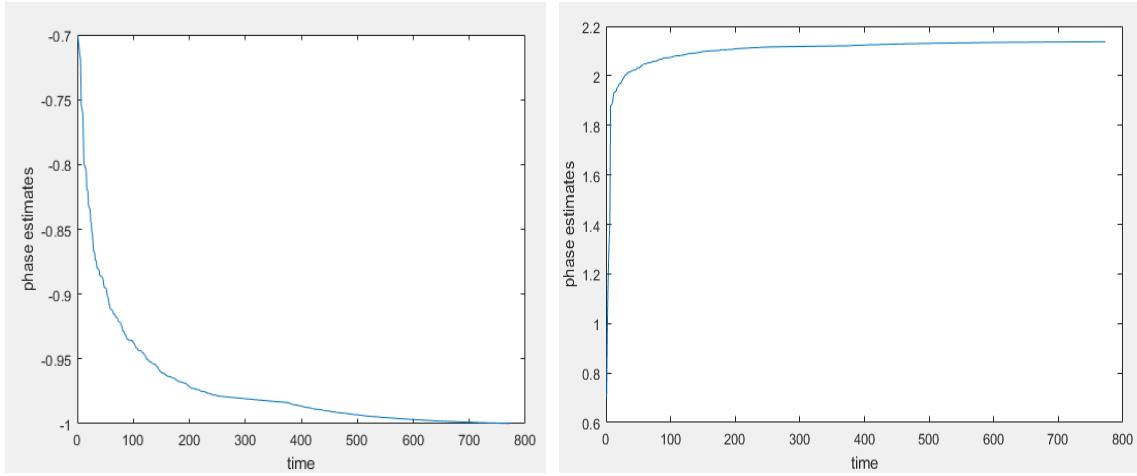


Figure 10: Convergence of phase tracking by decision directed method, initial estimates -0.7 and 0.7 respectively while phase offset is -1

4.4 Correlator

The method used on the receiver side both to maximize the SNR value while receiving a pulse to find location of pulses by finding maximum correlator output when the hamming pulse used in correlator completely overlap with signal pulses. Correlation is a kind of filter and for even symmetric signals correlation equals convolution. Since symmetry applies to the pulses, they provide this situation, so convolution is applied.

In this part, convolution is preferred to obtain the last symbol, we made room for the last symbol by applying zero padding. Since message shaped with hamming, correlation is achieved with hamming.

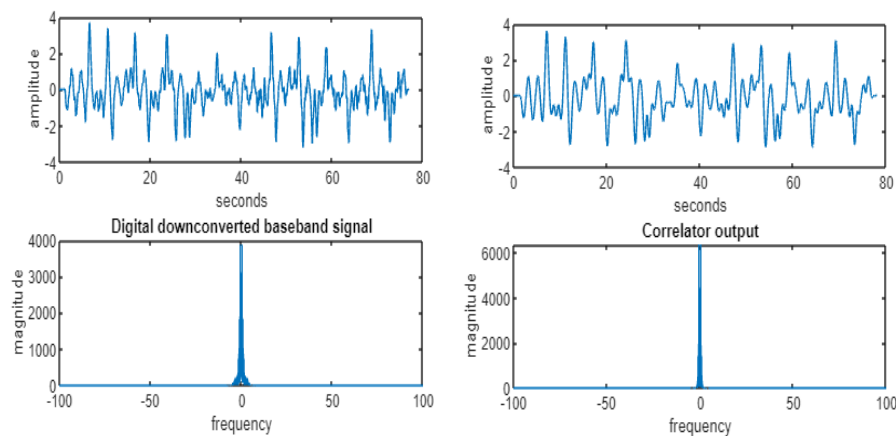


Figure 11: Effect of the correlator

When correlator operation is applied to the baseband signal, the results are as seen in the **Figure 11**, maximum correlation occurs at peak values and it is enhanced. Cleaner signal is obtained and SNR is improved.

Eye diagrams are one of the systematic methods which can be used to test how easily the pulse can be decoded or how accurately it can be transmitted. It is a graph obtained by projecting the pulses carrying symbols, one after the other. Then an eye figure is obtained, and it can be understood that the more open the eyes are, the more the symbols are clearly separated. This is an indication of how well the pulses sent to receiver will be decoded.

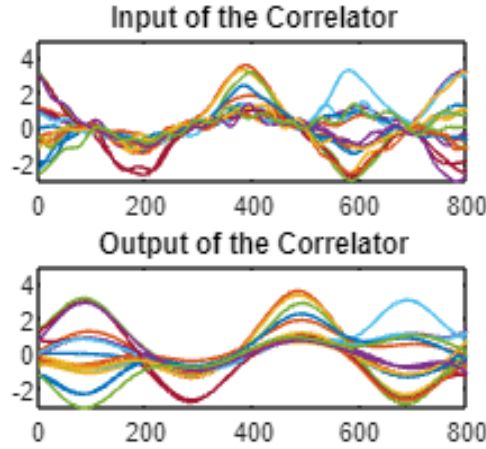


Figure 12: Eye diagrams at the input and the output of the correlator

As it can be seen in **Figure 12**, the correlator made the eyes open, and the noise decreased. A delay is observed in the graph, it is due to the firpm function we use when the carrier pulls the signal to the baseband after carrier synchronization and performs downconversion. Obtained baseband signal is delayed using a linear filter by 100 sample because of this filter with 200 sample length due to group delay of filter [6].

The purpose of the pulse shaping process is to use as wide a pulse as possible because this will enable us to use less region in the pulse frequency domain, but this wide pulse can create problems such as intersymbol interference in pulses with consecutive symbols. For example, when trying to expand the pulse, overlap situations can be observed in the Hamming pulse.

4.5 Downsampling and Time Synchronization

The reason behind the interpolation in timing recovery is because signal is shifted, and for downsampling, correct points of symbols are required to have soft decisions. There may also be points that is not a peak sample due to shifting. Timing synchronization is required to find peak samples.

$$J_{cv}(\tau) = \frac{1}{N} \sum_{k=k_0}^{k_0+N-1} \{(Q(x[k]) - x[k])^2\} = \text{avg}\{(Q(x[k]) - x[k])^2\} \quad \text{Eq. 10}$$

As a cost function of baud timing, we considered decision-directed method that us derived from cluster variance first. It can be seen in **Equation 10**; cluster variance can be

calculated by subtracting squared of $x[k]$ from quantized $x[k]$ and taking its average. It helps us to show how much the constellation diagram deviates from the symbols. Tau is tried to be found by minimizing the error here. Again, using the steepest descent algorithm and derivation, desired tau can be reached.

$$\tau[k + 1] = \tau[k] + \mu(Q[k] - x[k]).(x\left(\frac{kT}{M} + \tau[k] + \delta\right) - x\left(\frac{kT}{M} + \tau[k] - \delta\right)) \quad \text{Eq. 11}$$

When the necessary expressions are written instead, our algorithm turns into **Equation 11**. In order to perform this algorithm, we have a problem which is that we have samples at the time $(kT/M + \tau)$ but have not when δ is added and subtracted. The way to find these samples is to apply interpolation. It has been possible to realize the interpolation method (intersinc function) applied by using some of the incoming samples and using a linear filter with a truncated sinc response and find the optimum t . Hamming pulses length correspond to the spaces between our symbols. So, in order to add our leading and trailing pulses, this will be done for each symbol, starting with just f_l+1 and shifting.

The intersinc function also helps to find the symbols $t_{now} + \tau + \delta$ and $t_{now} + \tau - \delta$. Then, derivative and quantize operations are applied in the loop. t_{now} is then updated by M in every cycle. The updated version is also saved into $tausave$ and what is expected is that this convergence of the algorithm to time offset (t_offset). T_offset is implemented as 0.3.

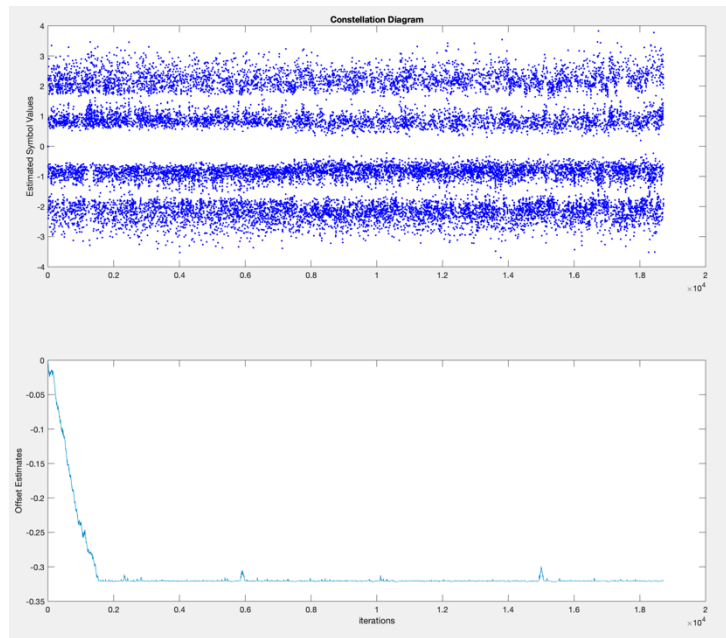


Figure 13: Convergence of the time offset

The algorithm converges to the negative state of the time offset to bypass it, after that there is no offset in between. As seen in **Figure 13**, errors occur in the constellation diagram until it converges to the correct value.

Our second cost function is based on output power maximization. Samples are squared and average of the squares are calculated, which corresponds the average output power. The reason it is preferred is the peak points of the pulses exactly coincide with the symbols, so when we take the frames and add them, the larger it can be, the more we can bypass this timing offset. The difference from the previous method is that the - sign in the previous formula is + here because the error function used here is to be maximized.

$$\tau[k+1] = \tau[k] + \mu \frac{\partial}{\partial t} [\text{avg}\{x^2[k]\}]|_{\tau=\tau[k]} \quad \text{Eq. 12}$$

This algorithm has taken a more straightforward approach, the symbols are shifted by interpolating according to the change of τ . The resulting convergence of the time offset via output power maximization method is as in **Figure 14**.

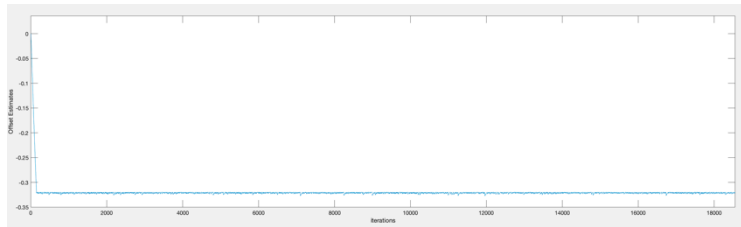


Figure 14: Convergence of the time offset with output power maximization method

It has been observed that the decision-directed method cannot converge correctly to the time offset when the signal from the transmitter suffers from excessive and flat fading.

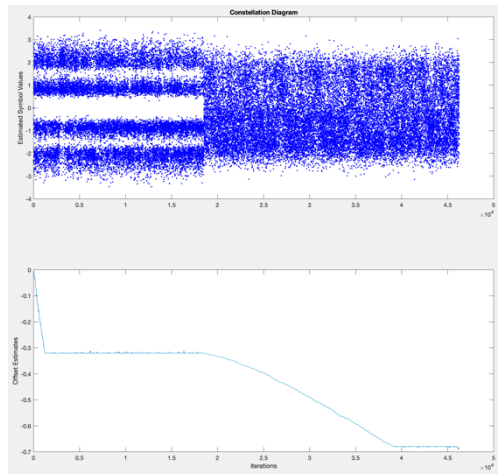


Figure 15: Effect of the flat fading on time recovery

In **Figure 15**, it is seen that the converge behavior has changed since the flat fading started. AGC converges to the desired magnitude after some time and until the magnitude of the samples are not correct since presence of fading. Decision directed method includes quantization and at the moment fading starts. Quantization cannot be performed successfully since AGC convergence could not be achieved yet. The reason for this is that the cluster variance used in the decision directed method cannot produce correct results within the presence of fading. Therefore, in this project, output power maximization method will be used for time recovery.

4.6 Decision

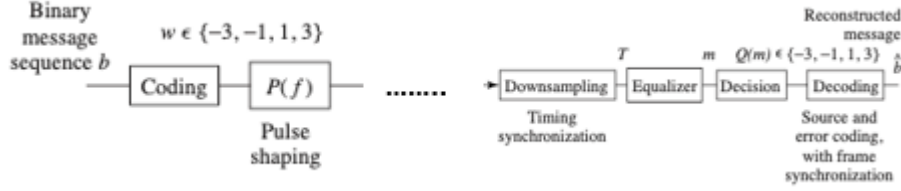


Figure 16: Labels the signals at various points [7]

In digital systems, the received message must be attained to a value in the symbol alphabet. For this, the nearest neighbour method is used to quantify the soft decision and determine the hard decision. The nearest neighbor method,

$$Q(m(kT)) = \min ((m(kT) - [\text{alphabet symbols}])^2) \quad \text{Eq. 13}$$

gives the nearest symbol. In addition, symbols of the alphabet change according to modulation order e.g. if modulation order is 4, the alphabet is [-1-3,1,3].

In this step, various error metrics were used to observe the quality of the system. Firstly, the average squared symbol recovery error,

$$\frac{1}{M} \sum_{k=1}^M (w(kT) - m(kT))^2 \quad \text{Eq. 14}$$

used to measure the error between the message at the transmitter side and the soft decision. In addition, the average squared hard decision error,

$$\frac{1}{M} \sum_{k=1}^M (w(kT) - Q\{m(kT)\})^2 \quad \text{Eq. 15}$$

is found by taking the difference between the message signal and the quantized signal. With the cluster variance,

$$\frac{1}{M} \sum_{k=1}^M (Q\{m(kT)\} - m(kT))^2 \quad \text{Eq. 16}$$

the error between the soft decision and the hard decision is found. Beyond that, there are also other indicators to measure the performance of the system. One of them is bit error rate (BER),

$$c(kT_b) = \begin{cases} 1 & \text{if } b(kT_b) \neq \hat{b}(kT_b) \\ 0 & \text{if } b(kT_b) = \hat{b}(kT_b) \end{cases}, \quad BER = \frac{1}{M} \sum_{k=1}^M c(kT_b) \quad \text{Eq. 17}$$

used to get rate of how many bits have been incorrectly received.

The other is symbol error rate (SER),

$$c(kT) = \begin{cases} 1 & \text{if } w(kT) \neq Q\{m(kT)\} \\ 0 & \text{if } w(kT) = Q\{m(kT)\} \end{cases}, \quad SER = \frac{1}{M} \sum_{k=1}^M c(kT) \quad \text{Eq. 18}$$

used to get rate of how many alphabet symbols have been incorrectly received. All of the mentioned error metrics were used in this project to observe the performance of the system. In Results section, the results of these metrics are also given for the different system configurations tried.

4.7 Decoding

In order to transform the quantized message into the sent information, the decode process is performed. Different designs are made according to the message type to be sent. In this project text and RGB images are sent.

First, the symbols obtained as a result of quantization are demodulated according to the selected modulation order. For the message as image, the decimal numbers obtained are converted to binary. The output in a row is divided into groups of 8 because RGB holds 8 bits for each pixel. Thus, the decimal number corresponding to each 8-bit group is an RGB pixel value. In the absence of any situation that will decrease the performance of the system, the sent, and the decoded message are as in **Figure 17**.

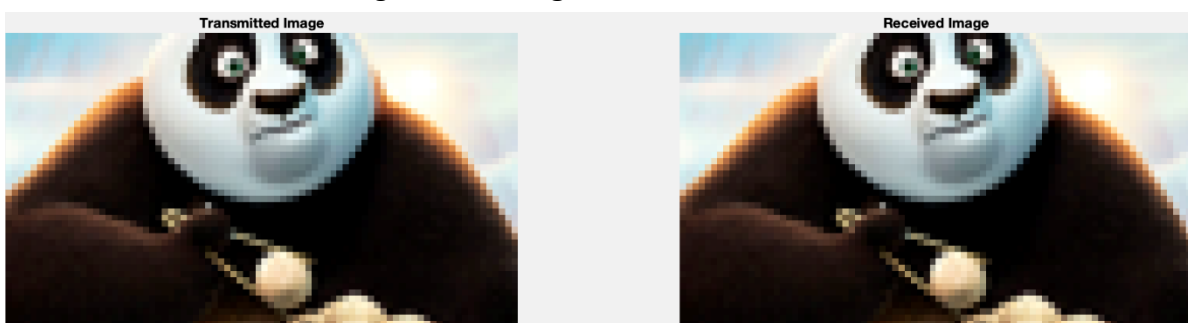


Figure 17: Transmitted and received images

5. Results

This section includes the performance analysis of the designed system. Various experiment sets were created to observe the behavior of the system. The metrics of the system are symbol recovery error, hard decision error, cluster variance, bit error rate (BER) and symbol error rate (SER). In every step, the transmitted and received images are given to maintain a visual error metric. There will also be constellation diagrams at the output of the downampler and the quantizer.

The experiment sets given below were carried out by changing the broadband noise and flat fading ratio. Scenarios were given and outputs were taken from the situation that affected the system the least to the situation that affected the system more. Time offset, phase offset, and narrowband noise are provided in all conditions.

5.1 Ideal System

Firstly, in the absence of any noise, time shift and carrier phase in the system, the ideal output is achieved. The parameters for ideal conditions are as in **Table 1**.

Table 1

Parameters	Values
Time Offset	0
Phase Offset	0
Broadband Noise	0
Narrow Band Noise	0
Flat Fading	0

As seen in **Table 2** for this case, the measured bit rate error, symbol rate error and hard decision error are 0, and cluster variance and symbol recovery errors are small enough to be accepted as 0, this small error is effect of AGC since PAM signals have changing amplitudes and it is discardable.

Table 2

Error Type	Measured Error
Symbol Recovery Error	0.000005
Hard Decision Error	0
Cluster Variance	0.000005
BER	0
SER	0

Besides, the eye diagram at the input of the correlator, output of the correlator, output of the downampler and the output of the quantizer can be seen in **Figure 18**. Detailly, just 3000 of the data at the input and the output of the correlator are shown for clarity. Most

importantly, the eyes are open, and constellations are not shift at the output of the downampler.

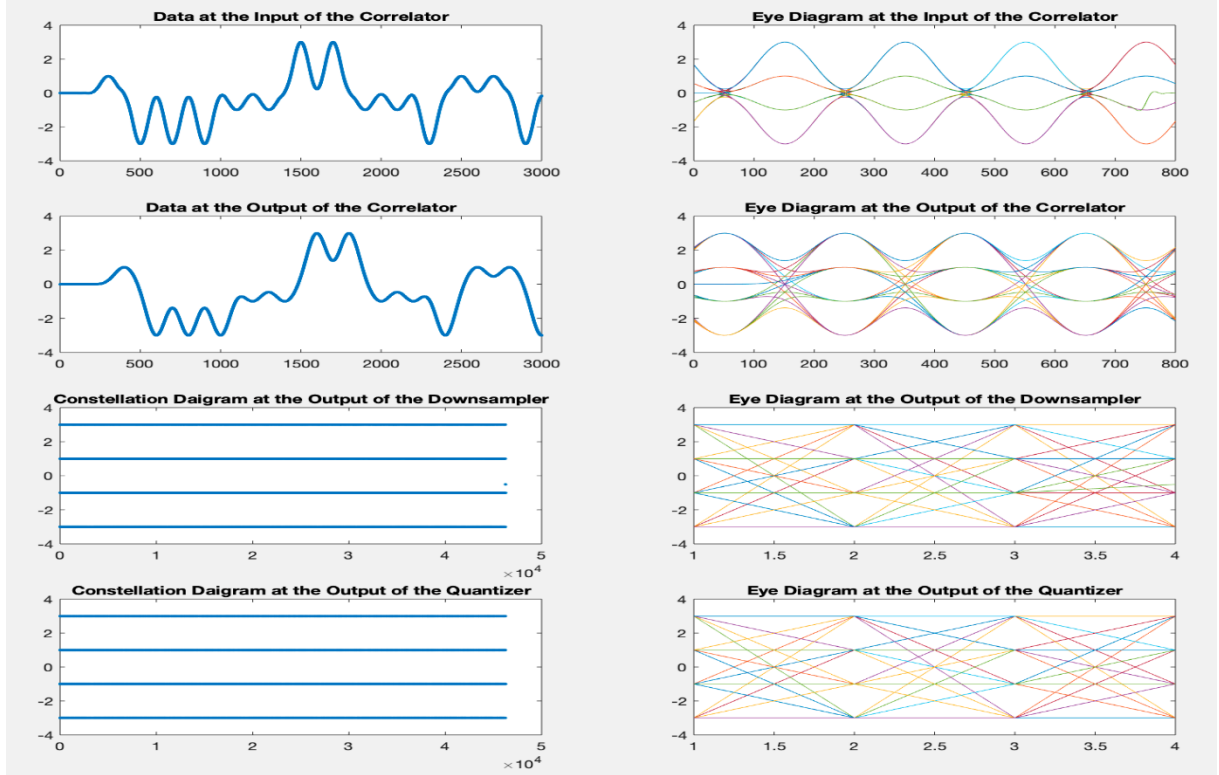


Figure 18: Soft and Hard decisions

The received image is in **Figure 19**. It is the same as the transmitted image because there is no bit error rate.

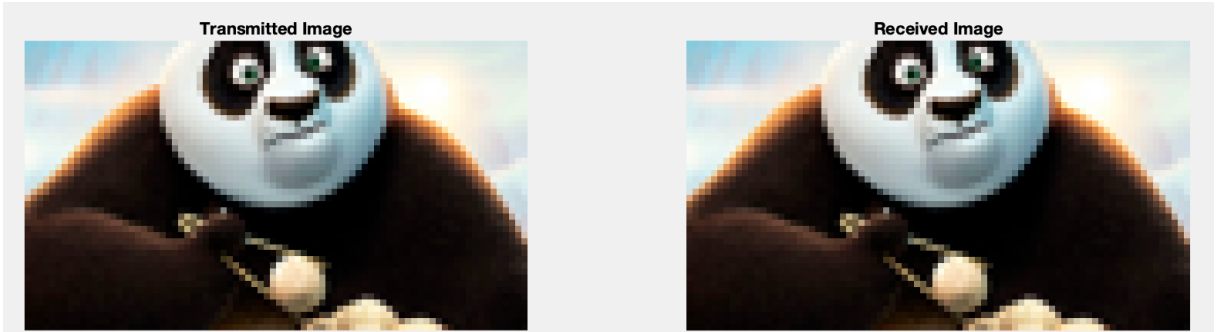


Figure 19: Transmitted and received images

5.2 Test for Easy Conditions

For this experimental setup, parameters that will affect the system performance slightly are selected. These parameters are shown in **Table 3**.

Table 3

Parameters	Values
Time Offset	0.3
Phase Offset	-1
Broadband Noise	0.2
Narrow Band Noise	2, randomly
Flat Fading	0.8 from 0.4 of the data

The error values measured for these conditions are as in **Table 4**.

Table 4

Error Type	Measured Error
Symbol Recovery Error	0.1536
Hard Decision Error	0.0078
Cluster Variance	0.1528
BER	0.0973 %
SER	0.1946 %

It is seen in **Figure 20** that the eyes in the eye diagram are more closed compared to the ideal system.

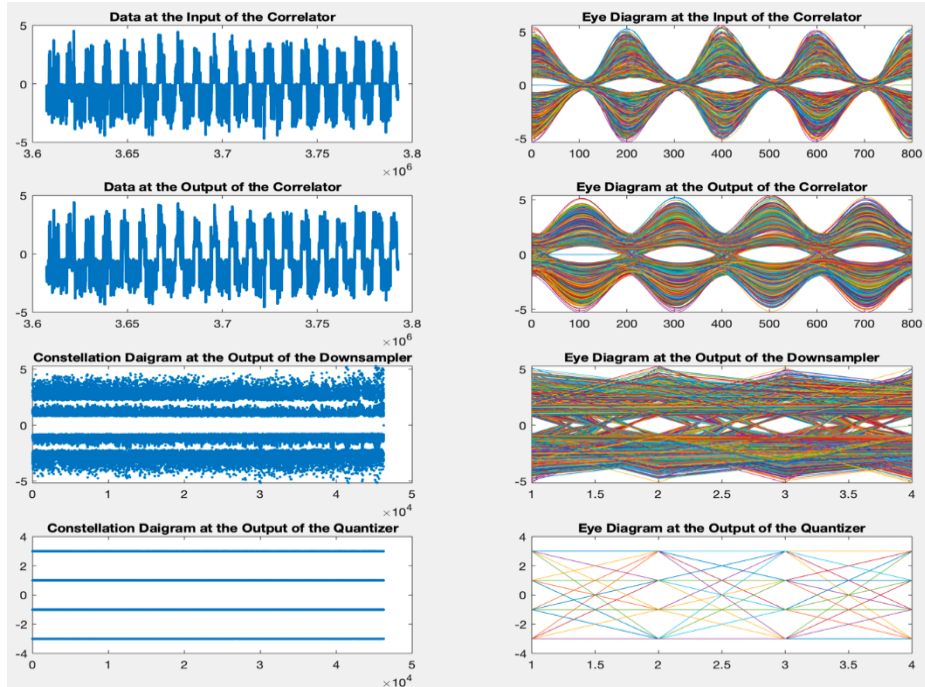


Figure 20: Soft and Hard decisions

The received image is in **Figure 21**, it doesn't be distinguished from the original transmitted image due to the small bit error rate.

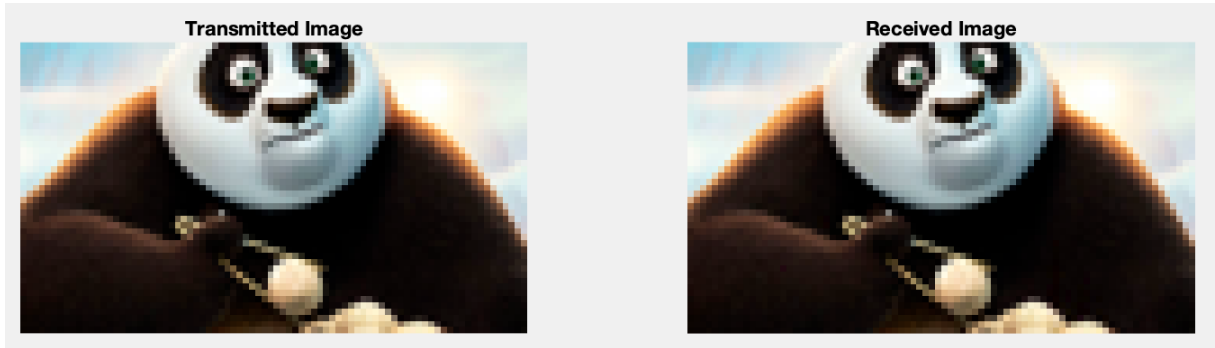


Figure 21: Transmitted and received images

5.3 Test for Medium Conditions

For this experimental setup, parameters that will affect the system performance averagely are selected. These parameters are shown in **Table 5**.

Table 5

Parameters	Values
Time Offset	0.3
Phase Offset	-1
Broadband Noise	0.5
Narrow Band Noise	2, randomly
Flat Fading	0.5 from 0.4 of the data

The error values measured for these conditions are as in **Table 6**. There has not been a noticeable increase in error values.

Table 6

Error Type	Measured Error
Symbol Recovery Error	0.1324
Hard Decision Error	0.0038
Cluster Variance	0.1320
BER	0.0476 %
SER	0.0951 %

In **Figure 22**, it is seen that the eyes in the eye diagram are close to each other at the correlator entrance. In this step, the positive effect of the correlator is seen. Because, it was observed that the eyes were slightly opened at the output of the correlator.

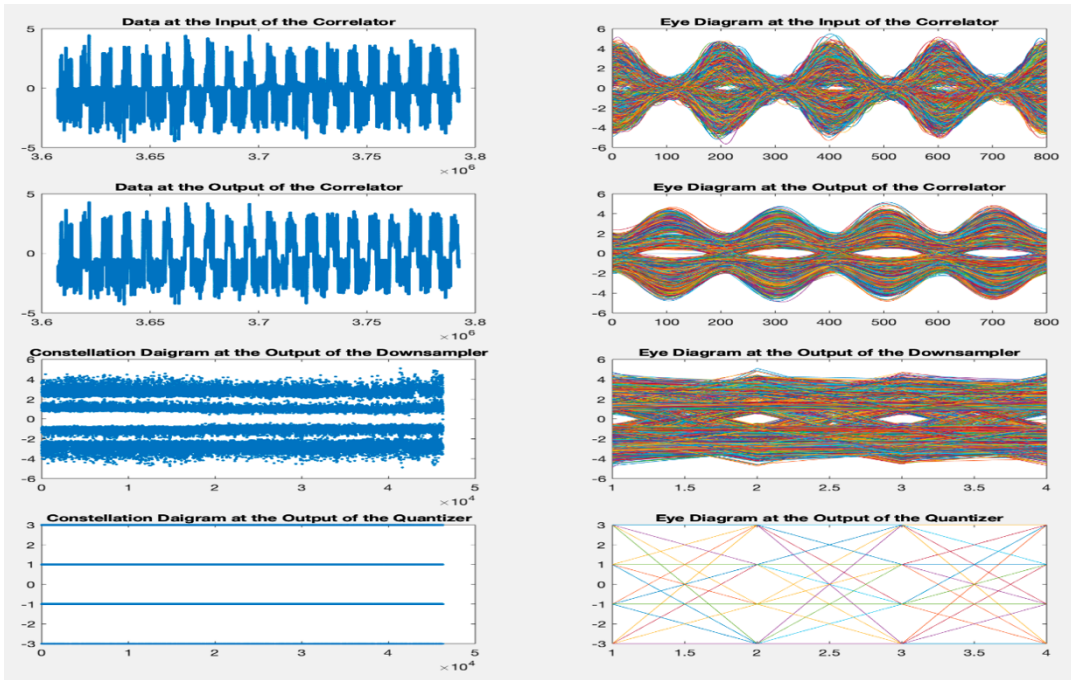


Figure 22: Soft and Hard decisions

The received image is in **Figure 23**, it doesn't be distinguished from the original transmitted image due to the small bit error rate.

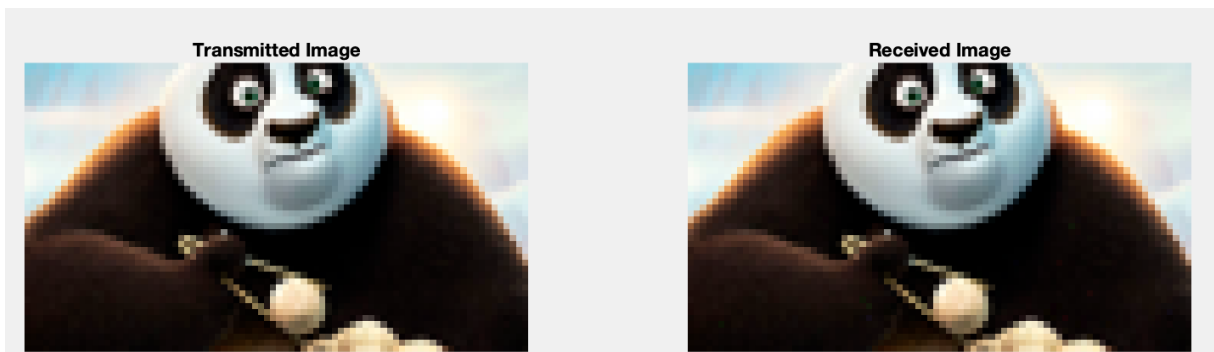


Figure 23: Transmitted and received images

5.4 Tests for Harsh Conditions

For this experimental setup, parameters that will affect the system performance harshly are selected. These parameters are shown in **Table 7**.

Table 7

Parameters	Values
Time Offset	0.3
Phase Offset	-1
Broadband Noise	0.8
Narrow Band Noise	2, randomly
Flat Fading	0.2 from 0.4 of the data

The error values measured for these conditions are as in **Table 8**. There has been a noticeable increase in error values.

Table 8

Error Type	Measured Error
Symbol Recovery Error	0.4980
Hard Decision Error	0.6827
Cluster Variance	0.2809
BER	9.4145 %
SER	17.0667 %

In **Figure 24**, it is seen that the eyes in the eye diagram are not open at all at the correlator entrance and exit.

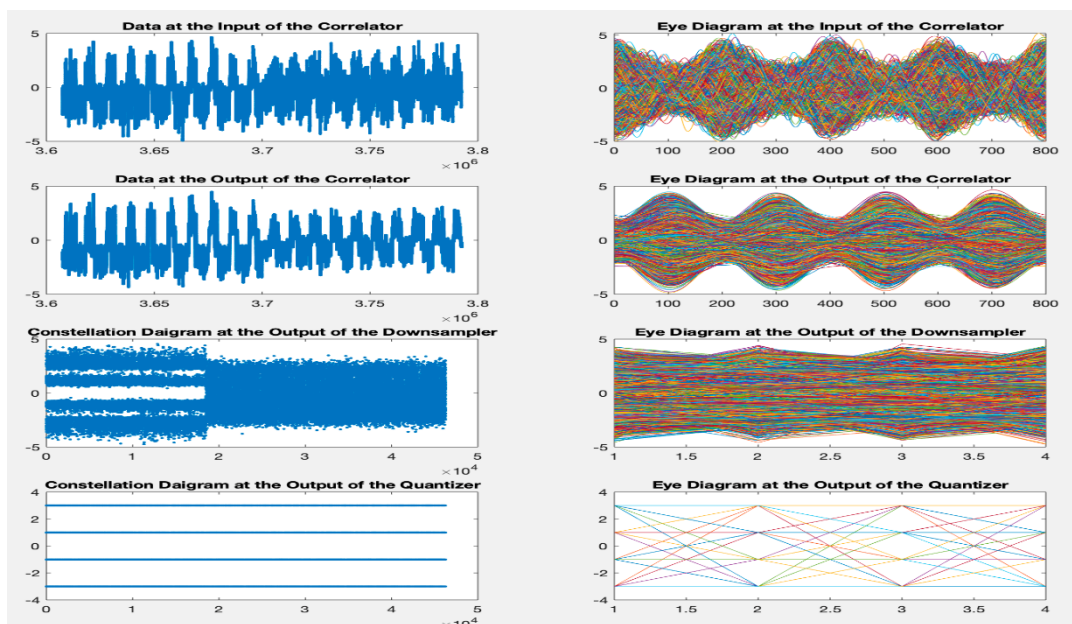


Figure 24: Soft and Hard decisions

Due to the high error rate, the distortions in the image shown in **Figure 25** have reached a visible level.

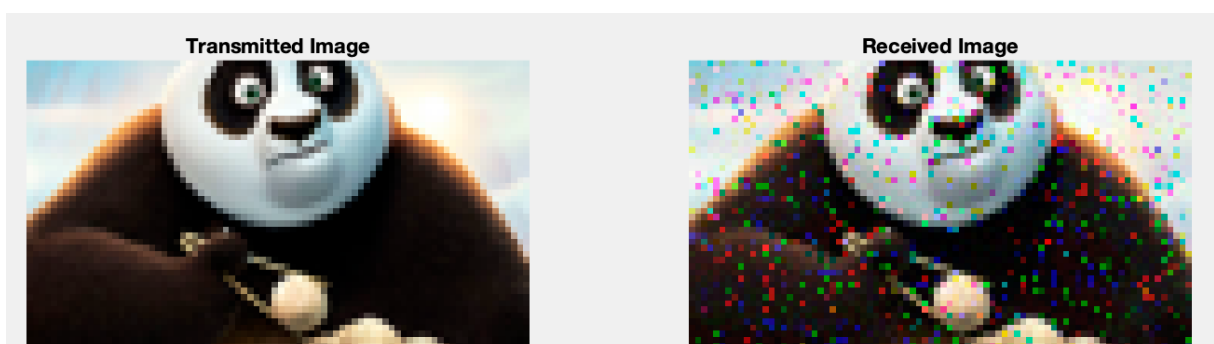


Figure 25: Transmitted and received images

5.4 Tests for Extreme Conditions

For this experimental setup, parameters that will affect the system performance extremely are selected. These parameters are shown in **Table 9**.

Table 9

Parameters	Values
Time Offset	0.3
Phase Offset	-1
Broadband Noise	1.5
Narrow Band Noise	2, randomly
Flat Fading	0.2 from 0.4 of the data

The error values measured for these conditions are as in **Table 10**. There has been a huge increase in error values.

Table 10

Error Type	Measured Error
Symbol Recovery Error	1.1961
Hard Decision Error	1.3966
Cluster Variance	0.2558
BER	20.2106 %
SER	34.3193 %

In **Figure 26**, it is seen that the eyes in the eye diagram are not open at all at the correlator entrance and exit.

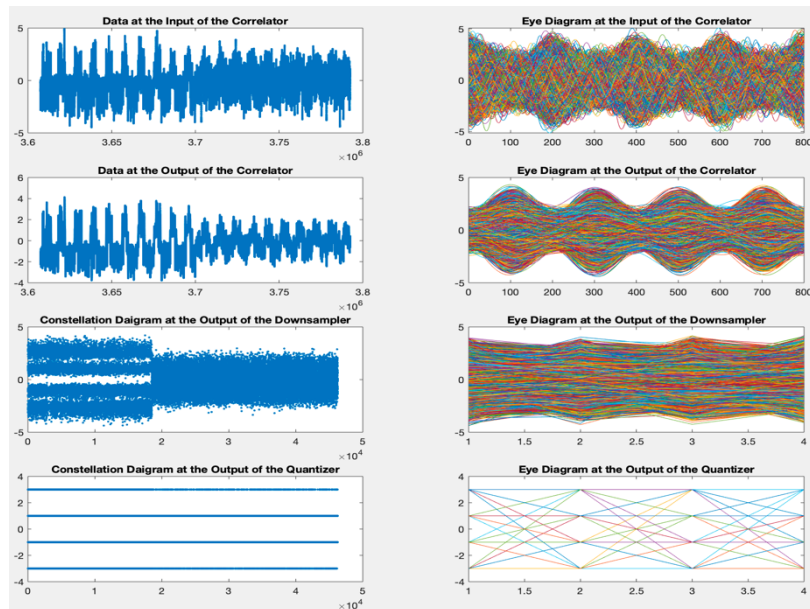


Figure 26: Soft and Hard decisions

Due to the high error rate, the distortions in the image shown in **Figure 27** have reached a visible level.

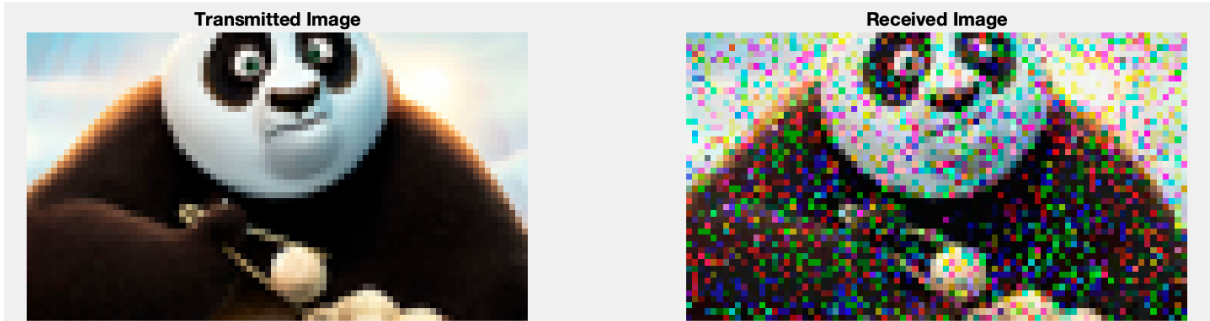


Figure 27: Transmitted and received images

6. Conclusion

Development of communication is mostly based on progresses in digital processing in recent years. Improvement in digital processing is provided flexibility with the implementation of software defined communication. In our project, we implemented a software defined radio by trying to realize challenges that is faced in reality like broadband noise, narrowband noise, flat fading, phase synchronization, timing offset.

During the project development period we tried to increase the number of challenges and blocks to overcome them as much as possible. Starting from Pulse Amplitude Modulation with 4 levels, most of the blocks that construct a software defined radio is used like bandpass filters to overcome the challenge of noise, AGC to overcome the fading effect, PLL and Decision direct to handle phase synchronization, and correlation to have accurate soft decisions in down sampler. Different error metrics like BER, SER, Cluster variance are used to measure effect of individual blocks and success of the algorithm.

Our aim in this project was being able to send an image, and text using constructed communication system. At the end of our project, we managed to achieve our aim with considerably low error rates as it is shown in the results using most of the blocks that we learned during lecture. Lastly, even if it was not possible to implement during development period until now, as an improvement, implementation of other real-life challenges like Multipath, Frequency synchronization, and solving them with Equalizer, Dual PLL can be done to simulate a more generalized radio. Also, raised cosine pulses can replace Hamming pulses to use bandwidth more efficiently beside channel and source coding methods.

We examined the results under 4 different circumstances that are easy, medium, harsh, and extreme conditions. As it is observed, there is no certain visual difference in between transmitted and received message for easy and medium conditions. In the harsh conditions, it is seemed that image is corrupted noticeably. Lastly, distortion on the image is significant in the extreme conditions by looking in **Figure 27** in related Result section.

References

- [1] M. N. O. Sadiku and C. M. Akujuobi, "Software-defined radio: a brief overview," *IEEE Potentials*, vol. 23, no. 4, pp. 14–15, 2004.
- [2] T. Ulversoy, "Software Defined Radio: Challenges and Opportunities," *IEEE Commun. Surv. Tutor.*, vol. 12, no. 4, pp. 531–550, 2010.
- [3] E. Grayver, *Implementing software defined radio*, 2012th ed. New York, NY: Springer, 2012.
- [4] "Fading basics," *Rfwireless-world.com*. [Online]. Available: <https://www.rfwireless-world.com/Articles/Fading-basics-and-types-of-fading-in-wireless-communication.html>.
- [5] "Received Signal Power," *Sciedirect.com*. [Online]. Available: <https://www.sciedirect.com/topics/engineering/received-signal-power>.
- [6] "What is Group Delay," *Iowahills.com*. [Online]. Available: <http://www.iowahills.com/B1GroupDelay.html>.
- [7] C. R. Johnson Jr, W. A. Sethares, and A. G. Klein, *Software receiver design: Build your own digital communication system in five easy steps*. Cambridge, England: Cambridge University Press, 2012.